Catalysis Science & Technology

Accepted Manuscript

ROYAL SOCIETY OF CHEMISTRY

www.rsc.org/catalysis

Journal Name

ARTICLE

Enhanced Catalytic Activity of Cobalt Catalysts for Fischer–Tropsch Synthesis via Carburization and Hydrogenation and Its Application for Regeneration

Received 00th January 20xx,
Accepted 00th January 20xx

DOI: 10.1039/x0xx00000x

www.rsc.org/

Geunjae Kwak, *[a] Du-Eil Kim, [a] Yong Tae Kim, [a] Hae-Gu Park, [a] Seok Chang Kang, [a] Kyoung-Su Ha, [b] Ki-Won Jun, [a] Yun-Jo Lee *[a]

In Fischer–Tropsch synthesis (FTS), cobalt carbide (Co_2C) is not a catalytically active material, but rather an undesired cobalt phase associated with low catalytic performance. It is known that Co_2C can be easily transformed back to metal cobalt in a H_2 environment at 220 °C. The transformed metal cobalt (hcp phase) even shows higher catalytic activity in low-temperature FTS, compared with the reduced cobalt metal from the cobalt oxide species. In this study, to obtain Co_2C with high catalytic behavior in FTS, we determined the optimum conditions for effective metal cobalt carburization and Co_2C hydrogenation by monitoring the phase transformation of cobalt using X-ray absorption spectroscopy (XAS) and temperature-programmed hydrogenation (TPH). We also verified that the transitions effectively occur under the same conditions as FTS (2.0 MPa, 220 °C). Based on the conditions determined for transitions, the deactivated cobalt catalyst can be completely regenerated in the FT reactor by simply altering the injected gases from syngas to CO and then H_2. Moreover, the regenerated catalyst shows enhanced catalytic performance compared with the fresh catalyst. The selective formation of hcp cobalt metal via carburization and hydrogenation of the spent catalyst was found to be the key for both the improved catalytic activity and the effective regeneration *in situ*. As a result, the formation of Co_2C, mainly considered a nuisance, could provide valuable applications in investigations of catalyst activation and regeneration in FTS.

1. Introduction

Fischer–Tropsch synthesis (FTS) converts synthesis gas (CO + H_2) into clean hydrocarbon fuels and valuable chemicals; much attention has been paid to the synthesis of environmentally benign fuels and chemicals from coal, biomass, and natural gas via syngas. The synthesis of liquid fuels via the gas-to-liquid route has attracted increasing interest because of the low price of natural gas, resulting from the increased development of unconventional gases (shale gas, coal-bed methane, and tight gas). Cobalt- and iron-based catalysts have been applied commercially in FTS processes [1–3]. Cobalt catalysts, in particular, are preferred for the production of transportation fuels due to the dominant coupling reaction between adsorbed hydrocarbon intermediates on the metal cobalt sites during FTS, the high per-pass conversion of synthesis gas, and their catalytic stability with a low deactivation rate [4].

Carbide is considered an important phase in commercial Fe and Co catalysts for FTS. Iron carbide is more active in FTS than metal iron and is the dominant phase of the two under FT reaction conditions [5]. Cobalt carbide (Co_2C), on the other hand, is not directly involved in FTS. Co_2C forms easily under a low H_2/CO ratio (< 1) and is considered a deactivation route of cobalt-based catalysts during FTS [6, 7]. It was initially proposed by Fischer and Tropsch that Co_2C is an intermediate for the growth of hydrocarbons during FTS [8], however, according to more recent studies, the carbide phase is neither an intermediate nor a catalytically active site for FTS [9, 10], and very stable under Fischer-Tropsch synthesis conditions. [7] Mohandas et al. [11] recently investigated that a fraction of carbide was reduced to a metal cobalt in a continuous stirred tank reactor under actual FTS conditions, but the cobalt carbide showed significantly low catalytic performance in FTS.

Interestingly, the inactive Co_2C in FTS can be readily converted back to metal cobalt at about 200 °C via hydrogenation [9, 10, 12, 13]. Claeys et al. [7] have also revealed that the carbide species decomposed in argon at 300 °C by using in situ magnetometer. The transformed cobalt metal phase mainly contains cobalt metal with a hexagonal close packed (Co_{hcp}) structure, which shows more active catalysis for CO hydrogenation than the cobalt face centered cubic (Co_{fcc}) structure obtained from the reduction of the cobalt oxide (Co_3O_4) phase over 400 °C [14–17]. The difference in activity between the hcp and fcc metal phases during FTS is caused by the intrinsic crystallographic structure and the corresponding morphology of Co_{hcp}, on which CO molecules can be easily

[a] Center for Carbon Resources Conversion, Korea Research Institute of Chemical Technology (KRICT), P.O. Box 107, Sinseongno 19, Yuseong, Daejeon 305-600, Republic of Korea.
[b] Nanoscale Catalysis and Reaction Engineering Lab, Department of Chemical and Biomolecular Engineering, Sogang University, 1 Shinsu-dong, Seoul, Republic of Korea.

Electronic Supplementary Information (ESI) available. See DOI: 10.1039/x0xx00000x

bound and dissociated [18, 19]. The presence of various favorable active sites leads to higher CO turnover rates in FTS. Recently, Liu et al. [20] theoretically verified that the direct dissociation of CO in the presence of H_2 readily occurs on the surface of Co_{hcp} via a direct dissociation route**.** In our recent study [21], we also reported that the transition of Co_2C to Co_{hcp} in H_2 occurs at a relatively low temperature of 220 °C. The reaction was monitored in detail using various *in situ* analyses, and Co_2C was found to be easily activated to Co_{hcp} in a slurry phase by H_2 bubbling. We also experimentally demonstrated that the *in situ* activated cobalt from Co_2C in the slurry showed higher catalytic activity in FTS than the *ex situ* reduced cobalt from Co_3O_4. The previous study focused on the low temperature transition of Co_2C and attempted to verify the fundamental phenomena related to the hydrogenation of Co_2C.

Herein, to achieve high catalytic performance in FTS, we verified the optimum conditions for obtaining, and then activating Co_2C by monitoring the transition of cobalt during carburization and hydrogenation, depending on the respective pressures. Additionally, we confirmed that the optimum conditions (2.0 MPa, 220 °C) concerning the transition of Co_2C can not only provide an advantage for low temperature activation with higher catalytic activity, but also broaden its applicability to the regeneration of spent catalyst. We experimentally confirmed that the catalytic activity of the deactivated Co catalyst could be restored, and even enhanced by a subsequent carburization-hydrogenation treatment under the same conditions as FTS (2.0 MPa, 220 °C). The Co_2C-based transitions during the course of the FT reaction can therefore be considered a more effective regeneration method because of its rapid transition, enhanced catalytic performance after the treatment, and convenient implementation.

2. Experimental

2.1. Catalyst preparation

A slurry impregnation method following our previous work [21] was used to prepare $CoPt/Al_2O_3$ catalyst with 23 wt% cobalt, promoted with 0.05 wt% Pt based on the reduced catalyst. Sasol Puralox-170 γ-alumina support was used as a catalyst support, while $Co(NO_3)_2{\cdot}6H_2O$ (> 97.0%, Samchun Pure Chemicals) and $Pt((NH_3)_2(NO_2)_2)$ (99.0%, Strem Chemicals) served as the Co and Pt precursors, respectively, in the loading solutions with ethanol as the solvent. A two-step slurry impregnation was applied to achieve the desired loading of Co. After each impregnation step, the catalyst was dried at 110 °C. After completing the Co addition, the Pt precursor solution was added to the catalyst by incipient wetness impregnation. The final catalyst was calcined under airflow at 400 °C for 5 h and was denoted $CoPt/Al_2O_3$.

2.2. Fabrication of Co_2C

The $CoPt/Al_2O_3$ catalyst was loaded into a conventional fixed-bed stainless-steel reactor and was supported by a layer of quartz wool. The $CoPt/Al_2O_3$ catalyst was pre-reduced in flowing 10% H_2/N_2 (6.0 L/(g_{cat}/h)) for 12 h at 400 °C and atmospheric pressure using a heating rate of 1 °C/min. After N_2 purging, the temperature was reduced, and carburization of the reduced catalyst was performed at 220 °C with a flow of pure CO (15 mL/$g_{cat.}$/min) for 5 h. Three samples were prepared using different CO pressures (0.1, 1.0, and 2.0 MPa). Before carburization, the degree of reduction of 71.9 % for the reduced $CoPt/Al_2O_3$ could be obtained by means of O2 titration of the reduced cobalt metal at 300 °C. The final carburized catalysts were carefully transferred to a vessel containing liquid squalene in a N_2-filled glove box to prevent air exposure. Before any form of characterization, filtering and drying of the soaked samples in air were performed.

2.3. Characterization

The prepared catalysts were characterized using various *ex situ* techniques. Powder X-ray diffraction (XRD) patterns were obtained at room temperature in the 2ϑ range from 10° to 80° using a Rigaku diffractometer with Cu Kα radiation to identify the crystalline phases of the cobalt species.

Temperature-programmed hydrogenation (TPH) was performed to determine the reduction and hydrogenation temperatures of the samples carburized at different pressures. Samples were pretreated by purging with He at 150 °C to remove traces of water. The TPH was performed using a 5% (v/v) H_2 in He at a flow rate of 30 mL/min. The catalyst samples were heated from 50 to 900 °C with a ramping rate of 10 °C/min.

X-ray absorption spectroscopy (XAS) measurements at the Co K-edge were performed at the 8C (Nano XAFS) beamline of the Pohang Light Source (PLS), Korea. The spectroscopic data were collected in a transmittance mode using gas-ionization detectors, and were calibrated by simultaneously measuring the spectrum of cobalt metal foil. The detailed XAS experimental method was reported in our previous study [21]. *In situ* XAS measurements on the Co K-edge were carried out using a gas manifold system and an *in situ* cell. Firstly, the $CoPt/Al_2O_3$ catalyst was reduced in the *in situ* cell in situ with a H_2 gas flow (20mL/min) at atmospheric pressure and 400 °C for 3 h. XAS spectra of the carburized samples were collected *in situ* with a CO gas flow (20 mL/min) at different pressures (0.1, 1.0, and 2.0 MPa) at 220 °C. XAS data reduction and fitting were carried out using WinXAS, FEFF, and IFEF-FIT software [22], and X-ray absorption near edge structure (XANES) spectra were obtained by normalization. Extended X-ray absorption fine structure (EXAFS) data were obtained by performing a Fourier transform.

2.4. Catalytic testing of Co_2C catalysts

FTS was examined over the Co_2C catalysts prepared under different CO pressures (0.1, 1.0, and 2.0 MPa) in a fixed bed reactor. The catalyst bed consisted of a 0.5 g sample diluted in 4.5 g of α-alumina powder, used to improve the isothermality of the reactor. Before the FTS tests, the catalysts were activated at 220 °C with 5% H_2/He for 2 h under atmospheric pressure. The flowing H_2 gas was then replaced by syngas ($H_2/CO/CO_2/Ar$ = 57.3/28.4/9.3/5.0 molar ratio) with a space velocity of 8.0 $L_{syn}/(g_{cat}/h)$ at 220 °C for FTS.

For comparison, FTS was performed with the $CoPt/Al_2O_3$ catalyst under normal activation conditions. The $CoPt/Al_2O_3$ catalyst was previously reduced with 5% H_2/He for 5 h at 400 °C. After that, the pressurized syngas ($H_2/CO/CO_2/Ar$ = 57.3/28.4/9.3/5.0 molar ratio) was introduced into the reactor, where the space velocity, reaction temperature, and pressure were 8.0 $L_{syn}/(g_{cat}/h)$, 220 °C, and 2.0 MPa, respectively.

Ar was used as the internal standard for the GC analysis of CO and the products. The effluent gas from the reactor was analyzed via online GC, using a GS-GASPRO capillary column connected to a FID (Flame Ionization Detector) for analysis of the hydrocarbons, and using a Porapak Q/molecular-sieve-packed column connected to a thermal conductivity detector. The conversions and selectivities towards hydrocarbons were calculated based on CO consumption and the selectivities were calculated on a carbon molar basis (details of the calculations are provided in the Electronic Supporting Information, ESI).

2. 5. Regeneration

The spent catalyst was regenerated by the carburization-hydrogenation treatment. Using 0.5 g of the reduced $CoPt/Al_2O_3$ catalyst, FTS was performed under the following conditions: 220 °C, 2.0 MPa, space velocity = 4.0 $L_{syn}/(g_{cat.}/h)$ and H_2/CO = 2 in a fixed bed reactor for more than 300 h. The deactivated catalyst with a lower FT activity than the initial value was treated with a CO gas stream of 10 mL/min at 220 °C and 2.0 MPa for 5 h. H_2 was subsequently passed inside the reactor at a flow rate of 30 mL/min at 220 °C, and 2.0 MPa for 2 h. After the regeneration steps, the performances of the regenerated catalysts were evaluated under the same conditions as the initial FTS.

3. Results and discussion

The XRD patterns of the catalyst samples carburized at different pressure levels, and the reduced $CoPt/Al_2O_3$ catalyst before carburization are shown in Figure 1. The samples were coated with liquid squalene to prevent air exposure before the XRD measurements. The peaks of the reduced $CoPt/Al_2O_3$ observed at 44.1 and 51.3° indicate the presence of Co_{fcc} (111) and Co_{fcc} (200) diffraction planes, respectively, which are

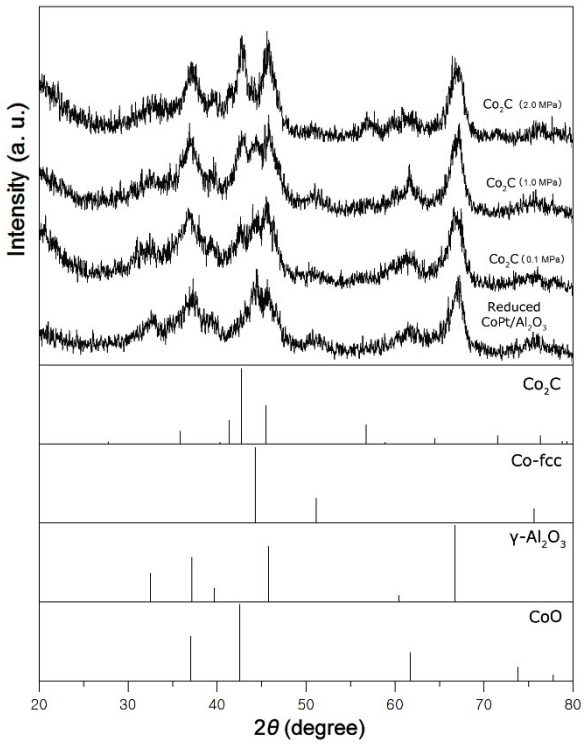

Figure 1. XRD patterns of Co_2Cs fabricated at different pressures (0.1, 1.0, and 2.0 MPa), and reduced $CoPt/Al_2O_3$.

typically obtained by reduction of the Co_3O_4 phase. These peaks gradually disappear with each increase in CO pressure at 220 °C, whereas new peaks corresponding to the Co_2C diffraction peaks (41.5° (020), 42.7 (111), and 45.7 (210), JCPDS card no. 050704) appear. In the samples prepared at CO pressures of 0.1 and 1.0 MPa, although the diffraction pattern depicts the presence of the Co_2C phase, the Co_{fcc} peaks remain, indicating that complete carburization did not occur. In addition, the diffraction peak at 62° was shown in Co_2C (0.1 MPa and 1.0 MPa), corresponding to the CoO (220) crystal plane (JCPDS, card no 09-0402). It can be inferred that the formation of CoO comes from the oxidation of insufficiently carburized cobalt in air exposure. On the other hand, CO treatment at 2.0 MPa was sufficient to form the Co_2C phase from Co_{fcc}. Presumably, it is preferable to dissociate the adsorbed CO molecules on the metal cobalt site at 2.0 MPa rather than at lower pressures because carbide formation between the dissociated surface carbon and the cobalt metal is enhanced. Previously, it was reported that a high pressure was required to maintain a steady state surface coverage of the chemisorbed CO before dissociation of the CO molecules for carburization [23]. Moreover, a relatively fast CO dissociation rate has also been experimentally observed at a pressure of 2.0 MPa during FTS [5], which is considered a suitable pressure for not only FTS, but also formation of the carbide phase.

Accordingly, the transition of reduced $CoPt/Al_2O_3$ to Co_2C is reflected in the pressure dependence of the normalized Co K-edge XANES spectra obtained by *in situ* XAS measurements, as shown in Figure 2. The shape of the reduced $CoPt/Al_2O_3$

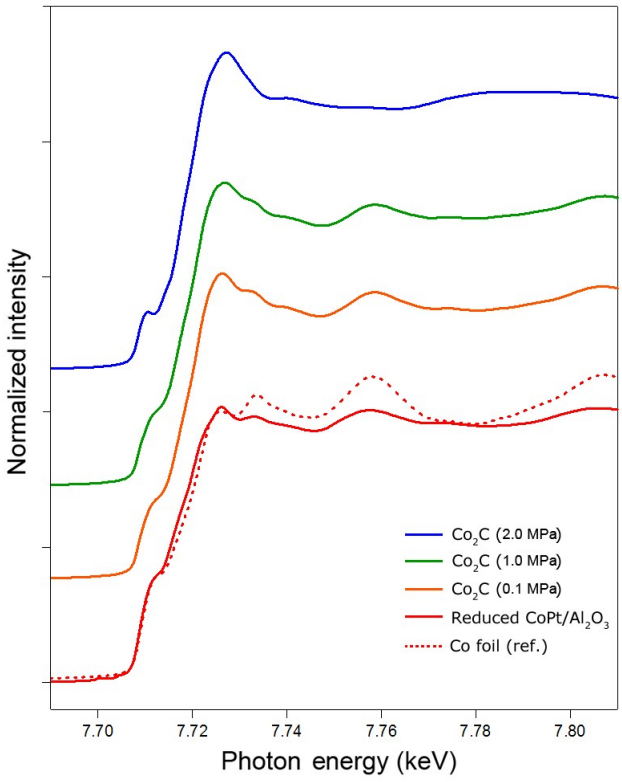

Figure 2.XANES profiles for reduced $CoPt/Al_2O_3$ and Co_2C samples after CO treatment at 0.1, 1.0, and 2.0 MPa, and reference standard (cobalt metal foil)

spectrum is almost consistent with that of the reference material (cobalt metal, red dotted line). The shape of the spectrum of the cobalt carburized at 2.0 MPa is different from that of the reference metal cobalt, but has similar features to previously reported spectra of carburized cobalt [11, 21]. The spectra shapes of the two samples prepared at lower pressures (0.1 and 1.0 MPa) show the coexistence of cobalt metal and carbide phases not fully carburized. Previous report also shows that the formation of bulk Co_2C was quite a slow process at atmospheric pressure because it requires the diffusion of carbon into the bulk metal cobalt [7]. It can be observed that the shape of the reduced $CoPt/Al_2O_3$ spectrum changes significantly with each increase in CO pressure. As a result, the Co_2C phase is well developed at a carburization pressure of 2.0 MPa under a CO atmosphere; these results are consistent with the XRD results.

The pressure-dependent evolution of Fourier transforms of k^1-weighted EXAFS at the Co K-edge for the reduced $CoPt/Al_2O_3$ under carburization conditions is also shown in Figure 3. The effect of carburization pressure on the transition of metal cobalt to Co_2C showed entirely close features to the results obtained from XANES. The Fourier transform of the EXAFS spectra indicate a common dominant peak at ~2.2 Å for the reduced $CoPt/Al_2O_3$ (red solid line), a typical bond distance from Co–Co scattering as found in Co foil (red dotted line). In the EXAFS spectra, the dominant peak gradually broadened as an increase of the carburization pressure and disappeared at 2.0 MPa of carburization pressure. The Fourier transforms of the Co_2C at 2.0 MPa consisted of two main peaks at 1.31 Å and 1.93 Å, which were assigned to Co–C and Co–Co coordination shells, respectively, in Co_2C [19, 22]. The metal cobalt was subsequently converted to the carbide state at 2.0 MPa, and was only present in trace amount, albeit lower in intensity, from the EXAFS spectra of the Co_2C (2.0 MPa) (blue solid line). In the case of the samples carburized at lower pressures (0.1 and 1.0 MPa), the Co–Co peak of the metal cobalt was still dominant accompanied by the gradual increase of the peaks corresponding to the Co_2C with increasing carburized pressure. From this result, we could speculate that the reduced $CoPt/Al_2O_3$ retained a metal phase up to 1.0 MPa; the metal cobalt phase was finally carburized to cobalt carbide at 2.0 MPa.

To confirm the extent of carburization for the three carburized cobalt samples, TPH was performed, as shown in Figure 4. It is known that the well-developed carbide phase shows a rapid transition to cobalt metal in a H_2 environment at a temperature of ~200 °C [7, 9–16, 24]. Consistent with these results, hydrogenation of the sample carburized at 2.0 MPa begins at ~160 °C and is complete at 250 °C, as shown in the TPH profile (blue line) in Figure 4. The single peak indicates the

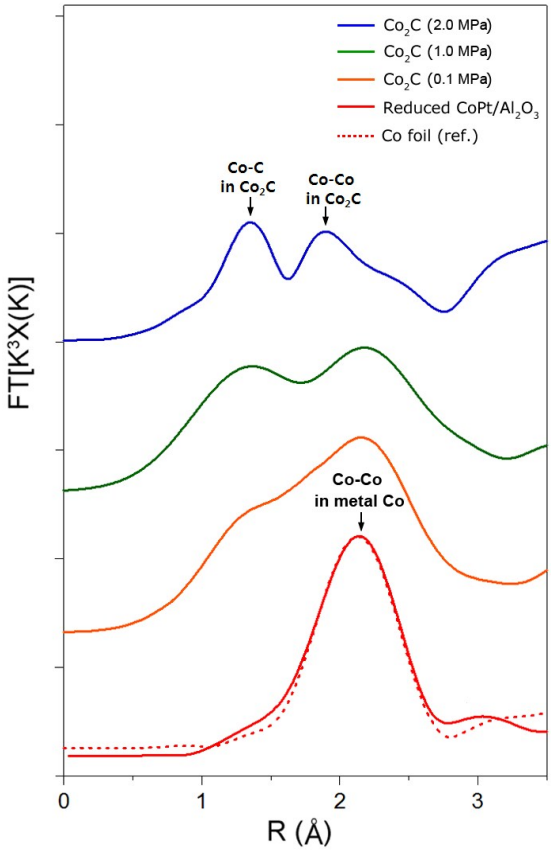

Figure 3. k^1-weighted EXAFS Fourier transform magnitude spectra of Co K-edge EXAFS spectra for $CoPt/Al_2O_3$ and Co_2C samples after CO treatment at 0.1, 1.0, and 2.0 MPa, and reference standard (cobalt metal foil).

transition of Co_2C to cobalt metal, and the shoulder below 200 °C implies the hydrogenation of oxygen-containing carbon species, such as carbonates and carbonyl compounds,

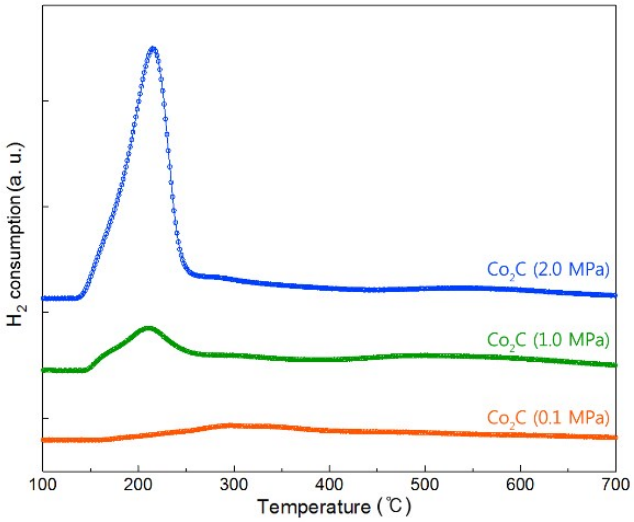

Figure 4. Temperature-programmed-hydrogenation (TPH) profiles for Co_2C catalysts carburized at different pressures (0.1, 1.0, and 2.0 MPa).

corresponding to adsorbed unreactive CO species [21]. According to previous work [25], carbonyl ligands begin to desorb between 90 and 160 °C, which is consistent with the temperature range of our shoulder peak. On the other hand, the amount of H_2 consumption significantly decreases with the decrease in the carburization pressure of the catalysts. In the case of the carbide samples prepared at 0.1 and 1.0 MPa, the peak and the shoulder corresponding to the carbide and the carbonyl compounds, respectively, gradually disappear with the decrease in carburization pressure. Moreover, the TPH peaks of Co_2C (sample prepared at 0.1 MPa) was not nearly detected, which might be was closed to the TPH feature of reduced cobalt metal before carburization. When the cobalt carburized at 0.1 MPa is exposed to air, an oxidation accompanied by an exothermicity was occurred instantly, indicating that the cobalt metal was not sufficiently carburized at 0.1 MPa. Consequently, a high CO pressure of 2.0 MPa is required for the sufficient transformation of metal cobalt to Co_2C. The higher pressure allows improved CO adsorption and dissociation on the metal cobalt by retaining a steady state surface coverage of CO molecules.

FTS was performed using the prepared carbide catalysts at 220 °C, 2.0 MPa, GHSV = 8.0 $L_{syn}/(g_{cat.}/h)$, and H_2/CO = 2 in a fixed bed reactor. For comparison, FTS with the $CoPt/Al_2O_3$ catalyst was performed under normal activation conditions (400 °C with 5% H_2/He for 5 h). The catalytic performance of each was evaluated in terms of CO conversion, catalytic time yields (CTYs), and hydrocarbon selectivities (Table 1). Co_2C prepared at 2.0 MPa shows the highest catalytic activity (CTY of 9.85 × 10^{-5} mol_{CO} g^{-1}_{Co} s^{-1} and C_{5+} selectivity of 86.7). The $CoPt/Al_2O_3$ catalyst shows a lower FT activity than Co_2C (2.0 MPa). This difference in the catalytic activities can be attributed to the structural difference between Co_{hcp} and Co_{fcc} derived from the carbide and oxide phases, respectively. The Co_{hcp} structure contains more defect sites and stacking faults, on which gas molecules are easily adsorbed with high binding energy. CO molecules can be more readily dissociated on the defect sites, leading to higher CO turnover rates in FTS, compared with the fcc structure. Previous studies [6, 14–17] have also suggested that cobalt catalysts containing the hcp cobalt phase show higher CTYs in FTS than cobalt catalysts containing the fcc phase; these reported results are in agreement with our results.

Table 1. Catalytic activities of cobalt catalysts in FTS. Co_2C catalysts were prepared using various carburization pressures (0.1, 1.0, and 2.0 MPa).

Catalyst (carburization pressure)	CO conversion (%)	CTY[a] [10^{-5} $mol_{CO}/(g_{Co}/s)$]	Hydrocarbon Selectivity (%)		
			CH_4	C_2–C_4	C_{5+}
Co_2C (2.0 MPa)	80.39	9.85	7.11	6.16	86.73
Co_2C (1.0 MPa)	71.86	8.80	7.31	6.71	85.98
Co_2C (0.1 MPa)	54.80	6.71	8.85	8.26	82.88
$CoPt/Al_2O_3$	75.32	9.22	8.56	8.17	83.27

* GHSV: 8.0 $L_{syn}/(g_{cat}/h)$, P: 2.0 MPa, T: 220 °C, H_2/CO ratio: 2.0, feed composition: $H_2/CO/CO_2/Ar$ = 57.3/28.4/9.3/5.0 (mol%). Co_2C catalysts and $CoPt/Al_2O_3$ were activated at 220 and 400 °C, respectively, with 5% H_2 (He balanced) for 5 h under atmospheric pressure. Catalytic properties were determined after 20 h on stream.

[a]Calculated from cobalt loading in catalysts, CO conversion, and GHSV

As expected, the Co_2C catalysts (0.1 and 1.0 MPa) that were insufficiently carburized show relatively lower FT activities (6.71 and 8.80 mol_{CO} g^{-1}_{Co} s^{-1}, respectively) and C_{5+} selectivities (82.88 and 85.98%, respectively), compared with Co_2C (2.0 MPa) and $CoPt/Al_2O_3$. This result indicates that the two Co_2C catalysts (0.1 and 1.0 MPa) have a reduced amount of Co_{hcp} transformed from the insufficiently carburized cobalt. Oxidation and burning of the remaining cobalt metal species (fcc) therefore occurs only partially, which can lead to lower CO turnover rates in FTS than the $CoPt/Al_2O_3$ catalyst. We also confirmed the partial oxidation of the two catalysts with less Co_2C formation, when exposed to air, in XRD patterns (Figure S1 in ESI). Consequently, to obtain the well-developed Co_2C, the reduced cobalt should be carburized at a pressure above 2.0 MPa in a CO atmosphere. In addition, the Co_2C (2.0 MPa) was successfully transformed to the cobalt metal hcp phase after the hydrogenation, shown in Figure S2 in ESI.

Moreover, analysis of the hydrogenation conditions shows that under H_2 at 220 °C, the well-developed Co_2C is easily converted to Co_{hcp}, at 2.0 MPa and atmospheric pressure (see Table S1 in ESI). The catalysts hydrogenated at different pressures show almost identical catalytic performances. The non-hydrogenated Co_2C, however, shows lower and more deteriorated FTS activities than the two hydrogenated catalysts. It is clear from these results that the hydrogenation step at atmospheric pressure or 2.0 MPa is desperately needed to obtain the enhanced catalytic activity.

The above results imply that the carbide phase was successfully employed as an intermediate for the regeneration of the used cobalt catalyst. Since carburization and hydrogenation can be performed at the same pressure as FTS (2.0 MPa), the carbide phase can be easily formed from deactivated metal cobalt, and subsequently transformed to active Co_{hcp} during FTS by simply changing the injected gas from syngas to CO and then H_2. To verify the ability of Co_2C-based regeneration to restore catalytic performance, carburization and hydrogenation treatments were applied to the spent catalyst after FTS reaction. The $CoPt/Al_2O_3$ used here

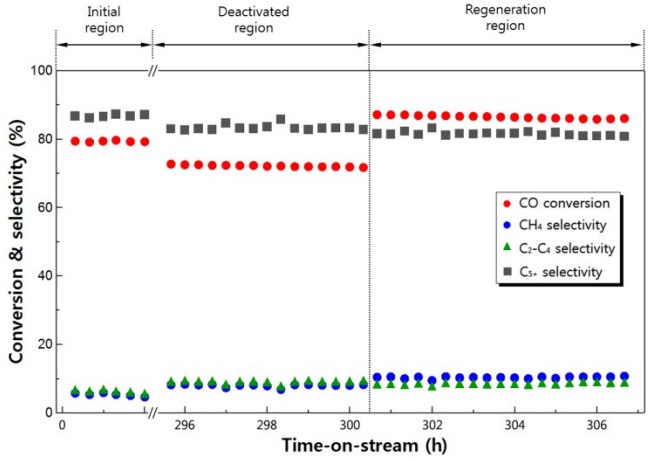

Figure 5.Changes in CO conversion and hydrocarbon (CH_4, C_2-C_4, and C_{5+}) selectivity with time-on-stream for initially activated (fresh) and deactivated (spent) cobalt catalysts, and regenerated catalyst after in situ carburization and hydrogenation at 220 °C.

was first reduced to metal cobalt in H_2 at 400 °C. FTS was then performed under the following conditions: 220 °C, 2.0 MPa, GHSV = 4.0 $L_{syn}/(g_{cat.}/h)$, and H_2/CO = 2 in a fixed bed reactor for more than 300 h. As shown in Figure 5, the regenerated catalyst is not only successfully restored, but its catalytic activity is improved, and is superior to the fresh catalyst. The recovered catalyst with relatively higher FTS activity can be attributed to selective formation of the Co_{hcp} during carbide hydrogenation. Previous studies [6, 14–17] have suggested that cobalt catalysts containing Co_{hcp} show higher CTYs in FTS than cobalt catalysts containing mainly Co_{fcc}; these reported results can be applied to and are in agreement with our results. However, it should be noted in Figure 5 that the methane selectivity increased somewhat from 5.96 % for fresh catalyst to 10.12 % for the recovered catalyst. The cause of increasing methane selectivity after the decarburization of Co_2C is unknown, but it might be speculated that Co_{hcp} might be implicated in previous study [7]. A complete understanding of higher methane production on the hydrogenated Co_2C in FTS will require further investigation.

Generally, the deactivated cobalt catalyst is regenerated following a complicated process: unloading the deactivated catalyst, dewaxing by washing, oxidation, and reduction at over 350 °C [26–29]. Due to the temperature difference between FTS and regeneration, the method requires additional equipment in which the washed catalyst can be oxidized and re-reduced, leading to additional costs for plant components. In comparison with conventional regeneration methods, our method provides a facile route leading to higher catalytic performance in FTS, and takes place in the FTS reactor without additional regeneration equipment. Furthermore, it is expected that Co_2C-based regeneration can be applied in slurry-phase FTS because of the low temperature required for regeneration. The deactivated catalyst in slurry-phase FTS can be easily restored *in situ* by CO and H_2 bubbling through the slurry at 220 °C, without thermal damage or deformation of the liquid medium in the slurry. The applicability of Co_2C to slurry-phase FTS has already been verified in our previous work [21].

Under realistic FTS conditions, sintering, carbon deposition, and surface reconstruction have been postulated as main causes of activity decline in the extended FTS run [23]. Even if not all of the major deactivation mechanisms can be reversed through Co_2C-based regeneration procedures, our regeneration method can simply overcome the deterioration of catalytic activity via the surface reconstruction required to transform to Co_{hcp}. Furthermore, Co_2C-based regeneration provides a facile route without altering significant process variables, and shows enhanced catalytic performance compared with that of the fresh catalyst.

4. Conclusions

We confirmed that carburized cobalt was optimally obtained by the treatment of metal cobalt in pure CO at 2.0 MPa, and the obtained Co_2C could be transformed to Co_{hcp} under H_2 flow at both 2.0 MPa and atmospheric pressure. Thus, the optimum pressure for carburization and hydrogenation was the same as that of FTS. At carburization pressures below 2.0 MPa, the catalytic activity decreased, and it was confirmed that the difference arose from the extent of Co_{hcp} derived from the carburized cobalt catalyst. We attempted to verify the extent of Co_2C in the cobalt catalysts carburized at varying pressures and monitor the evolution of Co_2C during hydrogenation, using XAS and TPH. Under the determined optimum transition conditions (220 °C and 2.0 MPa), the deactivated cobalt catalyst could be successfully regenerated to regain, and even surpass the initial catalytic activity by simple carburization and hydrogenation, resulting from the Co_{hcp} generated from the hydrogenation of Co_2C. Consequently, the present method can be considered to be a more effective regeneration method, because of its simplicity and the resulting enhanced catalytic performance.

Acknowledgements

This work was supported by Korea Institute of Energy Technology Evaluation and Planning (KETEP) under “Energy Efficiency & Resources Programs” (Project No. 2013201020178B) of Ministry of Knowledge Economy, Republic of Korea. This work was further financially supported by the core KRICT project (KK1501-B00) from Korea Research Institute of Chemical Technology and C1 Gas Refinery Program

through the National Research Foundation of Korea (NRF) funded by the Ministry of Science, ICT & Future Planning (2015M3D3A1064901).

References

1. R. Oukaci, A. H. Singleton, J. G. Goodwin Jr., *Appl. Catal., A*, **186**, 1999, 129–144.
2. M. E. Dry, *Catal. Today*, **71**, 2002, 227–241.
3. B. H. Davis, *Top. Catal.*, **32**, 2005, 143–168.
4. A. Y. Khodakov, W. Chu, P. Fongarland, *Chem. Rev.*, **107**, 2008, 1692–1744.
5. H. Schulz, *Appl. Catal.*, *A*, **186**, 1999, 3–12.
6. M. Sadeqzadeh, H. Karaca, O. V. Safonova, P. Fongarland, S. Chambrey, P. Roussel, A. Griboval-Constant, M. Lacroix, D. Curulla-Ferré, F. Luck, A. Y. Khodakov, *Catal. Today*, **164**, 2011, 62–67.
7. M. Claeys, M. E. Dry, E. van Steen, E. du Plessis, P. J. van Berge, A. M. Saib, D. J. Moodley, *J. Catal.*, **318**, 2014, 193–202.
8. F. Fischer, H. Tropsch, *Brennstoff Chem.*, **7**, 1926, 97–104.
9. S. Weller, L. J. E. Hofer, R. B. Anderson, *J. Am. Chem. Soc.*, **70**, 1948, 799–801.
10. R. B. Anderson, W. K. Hall, A. Krieg, B. Seligman, *J. Am. Chem. Soc.*, **71**, 1949, 183–188.
11. J. C. Mohandas, M. K. Gnanamani, G. Jacobs, W. Ma, Y. Ji, S. Khalid, B. H. Davis, *ACS Catal.*, **1**, 2011, 1581–1588.
12. S. Weller, *J. Am. Chem. Soc.* **69**, 1947, 2432–2436.
13. L. J. E. Hofer, E. M. Cohn, W. C. Peebles, *J. Phys. Chem.*, **53**, 1949, 661–669.
14. H. Karaca, O. V. Safonova, S. Chambrey, P. Fongarland, P. Roussel, A. Griboval-Constant, M. Lacroix, A. Y. Khodakov, *J. Catal.*, **277**, 2011, 14–26.
15. L. J. E. Hofer, W. C. Peebles, *J. Am. Chem. Soc.*, **69**, 1947, 893–899.
16. O. Ducreux, J. Lynch, B. Rebours, P. Roy, P. Chaumette, *Stud. Surf. Sci. Catal.*, **119**, 1998, 125–130.
17. M. K. Gnanamani, G. Jacobs, W. D. Shafer, B. H. Davis, *Catal. Today*, **214**, 2013, 13–17.
18. K. M. Kemner, W. T. Elam, V. G. Harris, Y. U. Idzerda, J. A. Wolf, *J. Vac. Sci. Tech. B,* **14**, 1996, 3207–3209.
19. D. I. Enache, B. Rebours, M. Roy-Auberger, R. Revel, *J. Catal.*, **205**, 2002, 346–353.
20. J. X. Liu, H. Y. Su, D. P. Sun, B. Y. Zhang, W. X. Li, *J. Am. Chem. Soc.*, **135**, 2013, 16284–16287.
21. G. Kwak, M. H. Woo, S. C. Kang, H. G. Park, Y. Lee, K. Jun, K. Ha, *J. Catal.*, **307**, 2013, 27–36.
22. B. Ravel, M. Newville, *J. Synchrotron Radiat.*, **12**, 2005, 537–541.
23. G. A. Beitel, A. Laskov, H. Oosterbeek, E. W. Kuipers, *J. Phys. Chem.*, **100**, 1996, 12494–12502.
24. H. Karaca, J. Hong, P. Fongarland, P. Roussel, A. Griboval-Constant, M. Lacroix, K. Hortmann, O. V. Safonova, A. Y. Khodakov, *Chem. Commun.*, **46**, 2010, 788–790.
25. C. Huber, K. Moller, T. J. Bein, *Phys. Chem.*, **98**, 1994, 12067–12074.
26. A. M. Saib, D. J. Moodley, I. M. Ciobîcă, M. M Hauman, B. H. Sigwebela, C. J. Weststrate, J. W. Niemantsverdriet, J. van de Loosdrecht, *Catal. Today*, **154**, 2010, 271–282.
27. A. M. Saib, J. L. Gauché, C. J. Weststrate, P. Gibson, J. H. Boshoff, D. J. Moodley, *Ind. Eng. Chem. Res.,* **53**, 2014, 1816–1824.
28. M. M. Hauman, A. M. Saib, D. J. Moodley, E. du Plessis, M. Claeys, E. van Steen, *ChemCatChem*, **4**, 2012, 1411–1419.
29. T. Jermwongratanachai, G. Jacobs, W. D. Shafer, V. R. R. Pendyala, W. Ma, M. K. Gnanamani, S. Hopps, G. A. Thomas, B. Kitiyanan, S. Khalid, B. H. Davis, *Catal. Today*, **228,** 2014, 15–21.

Graphical Abstracts